Extensions to the Hybrid Method of Moments/Uniform GTD Formulation for Sources Located Close to a Smooth Convex Surface

Isak P. Theron, *Member, IEEE*, David B. Davidson, *Member, IEEE*, and Ulrich Jakobus, *Member, IEEE*

***Abstract*—In this paper, we present an extension to the uniform geometrical theory of diffraction (GTD) for reflection from smooth curved surfaces. This approach allows the source to be much closer to the reflecting surface than the conventional uniform GTD formulation and does not require a Hertzian dipole source. In essence, the field point is mirrored in the plane tangential to the specular (reflection) point; the incident field is then calculated at the mirror point and the uniform GTD reflection coefficients are used to mirror this field to the original field point. This formulation reduces exactly to the conventional uniform GTD if the incident field is ray optical. The application to a hybrid method of moments (MoM)/GTD code is outlined and results computed using this code are presented for a dipole radiating in the vicinity of a cylinder.**

***Index Terms*—Electromagnetic diffraction, geometrical theory of diffraction (GTD), method of moments, UTD.**

I. Introduction

THE geometrical theory of diffraction (GTD) and its uniform versions are a very efficient way to calculate the radiation patterns of antennas in the vicinity of large conducting structures. This formulation requires a known current distribution and one needs to use hybrid formulations such as the method of moments (MoM)/uniform GTD hybrid [1], [2] to calculate current related parameters such as coupling and input impedance. In order to model antennas mounted on masts, aircraft, etc., the uniform GTD part must also treat curved surfaces.

The uniform GTD solution for reflection from smooth curved surfaces has been studied in detail [3], [4]. This formulation uses a reflection coefficient to relate the incident and reflected fields at the specular point and uses ray optics to calculate the field at any required point. The validity of the underlying assumptions decreases as the source or field point approaches the specular point. Antennas mounted on masts, etc. will, in general, be in the region where the reflection coefficients are no longer valid.

For flat plates, the reflected field may be found from the mirror image of the source. In the case of curved surfaces it is not as straightforward. When only the source is in the immediate vicinity of the specular point one needs to use a radiation formulation as in [5]. This formulation gives the radiated field for a Hertzian dipole very close to a cylinder. However, in some cases it is not advisable to decompose the source into Hertzian dipoles. An example is the MoM/uniform GTD hybrid formulation [2] in which the MoM part uses triangular basis functions. (It is possible to use the formulation for dipole radiation and integrate these contributions over the basis function. This, however, would require ray tracing inside the integration, resulting in significant additional computational cost.) This paper presents an extension of the conventional formulation to treat these cases. In the next section, we summarize the hybrid formulation. The section thereafter develops a mirror formulation to account for the uniform GTD reflection from smooth convex surfaces and the final section shows some near-field patterns as well as a typical application.

Manuscript received November 13, 1998; revised March 6, 2000.This work was supported by the (South African) FRD/DTI THRIP program and Electromagnetic Software and Systems Pty (Ltd).

I. P. Theron and D. B. Davidson are with the Department of Electrical and Electronic Engineering, University of Stellenbosch, Stellenbosch, 7600 South Africa.

U. Jakobus is with the Institut für Hochfrequenztechnik, University of Stuttgart, 70550 Stuttgart, Germany.

Publisher Item Identifier S 0018-926X(00)05794-X.

II. MoM/GTD Hybrid Method

In the full MoM [1], [6] one typically solves a matrix equation

$$[Z][I] = [V] \tag{1}$$

where $[V]$ is a vector related to the excitation, $[I]$ a vector containing the unknown coefficients of the basis functions in the current expansion, and $[Z]$ the interaction matrix. For a current based formulation the elements of the interaction matrix may be written as

$$Z_{mn} = \int_S \int_{S'} \bar{t}_m(\bar{r}) \cdot \overline{\overline{G}}(\bar{r}, \bar{r}') \cdot \bar{b}_n(\bar{r}')\, dS'\, dS \tag{2}$$

where

- S — surface on which the current is flowing;
- $\overline{\overline{G}}(\bar{r}, \bar{r}')$ — Green's dyadic giving the field at $\bar{r}$ due to a dipole at $\bar{r}'$, $\bar{b}_n(\bar{r}')$ is the nth basis function (which may be either a section of a line current or a part of a surface current);
- $\bar{t}_m(\bar{r})$ — mth testing function.

If an additional scatterer treated with GTD is added to the problem the interaction matrix may be modified [1]

$$\tilde{Z}_{mn} = \delta Z_{mn} + Z'_{mn} \tag{3}$$

where δ is a shadowing coefficient which is zero if the test function lies in the shadow of the scatterer and unity otherwise. The additional term

$$Z'_{mn} = \int_S \int_{S'} \bar{t}_m(\bar{r}) \cdot \overline{\overline{G}}^{\mathrm{GTD}}(\bar{r}, \bar{r}') \cdot \bar{b}_n(\bar{r}')\, dS'\, dS \tag{4}$$

gives the interaction between the source and field functions that occurs via the scatterer. Here $\overline{\overline{G}}^{\mathrm{GTD}}(\overline{r}, \overline{r}')$ represents the GTD field at $\overline{r}$ due to a source at $\overline{r}'$ but with the direct term excluded. The direct term is accounted for in the MoM part of the interaction term. In the above, the GTD contribution must be integrated over both the source and field regions. This may become very inefficient, as calculating the GTD field will generally require potentially time-consuming ray tracing.

If the source and field positions are electrically far from the specular (reflection or diffraction) points, the GTD field will be relatively constant over the electrically small basis and testing functions. It may therefore be treated as constant, allowing simple evaluation of the integrals in (4). This, however, limits both the source and field positions. We use a modification of this technique whereby one integral is calculated and one approximated. The incident field is calculated from the integral over the complete basis function. This source field is then reflected to the center of the testing function using our "mirror formulation" (discussed in the next section) that allows the source to be arbitrarily close to the surface. If the total path from the source to the field point via the cylinder is long enough, the field at the testing function will be relatively constant. We may therefore approximate the outer integral over S in (4) by assuming that the integrand is constant.

Our implementation relies on using an arbitrary source rather than a Hertzian dipole. Thus, it requires a GTD formulation written in terms of reflection and diffraction coefficients. It is not possible to use the closed-form dipole formulation in [5] as is done in the hybrid formulation in [7]; in Hsu's work, the moment method part was limited to line currents with sinusoidal basis functions. Since these basis functions may be explicitly written in terms of Hertzian dipoles at the edges of line segments, the dipole GTD formulation was appropriate. To model metallic surfaces by the MoM, we use rooftop basis functions over triangular patch elements. These basis functions do not decompose as easily to Hertzian dipoles.

III. Reflection Formulation

The conventional uniform GTD formulation for smooth curved surfaces has been given by Pathak *et al.* [3]. In this formulation, the total field (superposition of direct and reflected field) at point $\overline{P}$ in the lit region may be written in terms of the incident field at the specular point $\overline{Q}$

$$\overline{E}(\overline{P}) \approx \overline{E}^i(\overline{P}) + \overline{E}^i(\overline{Q}) \cdot \overline{\overline{\mathcal{R}}} \sqrt{\frac{\rho_1^r \rho_2^r}{(\rho_1^r + s^r)(\rho_2^r + s^r)}}\, e^{-jks^r} \quad (5)$$

where $\overline{E}^i$ is the incident field, k the propagation constant and

$$\begin{aligned} \overline{\overline{\mathcal{R}}} &= \mathcal{R}_s \hat{e}_\perp \hat{e}_\perp + \mathcal{R}_h \hat{e}_\parallel^i \hat{e}_\parallel^r \\ \mathcal{R}_{s,h} &= -\sqrt{\frac{-4}{\xi^L}}\, \exp\left(-j\frac{1}{12}(\xi^L)^3\right) \\ &\quad \cdot \left\{ \frac{e^{-j\pi/4}}{2\sqrt{\pi}\xi^L}[1 - F(X^L)] + \hat{P}_{s,h}(\xi^L) \right\} \end{aligned}$$

with $\hat{e}_\perp$ the unit vector normal to the plane of incidence, and $\hat{e}_\parallel^i$ and $\hat{e}_\parallel^r$ the unit vectors normal to $\hat{e}_\perp$ and to the incident and reflected directions, respectively. The variables ξ^L and X^L as well as the special functions $\hat{P}_s(\xi^L)$, $\hat{P}_h(\xi^L)$ and $F(X^L)$ are defined in, for example, [3], [8]. The variables ρ_1^r and ρ_2^r denote the principle radii of curvature of the reflected wave, and s^r is the distance from the specular or reflection point to the field point. We will also use s^i, the distance from the source to the reflection point. All points mentioned above, such as $\overline{Q}$, are described in terms of the vector from the origin to the particular point. When the source is too close to the specular point the incident field is no longer ray optical and the formulation as given fails.

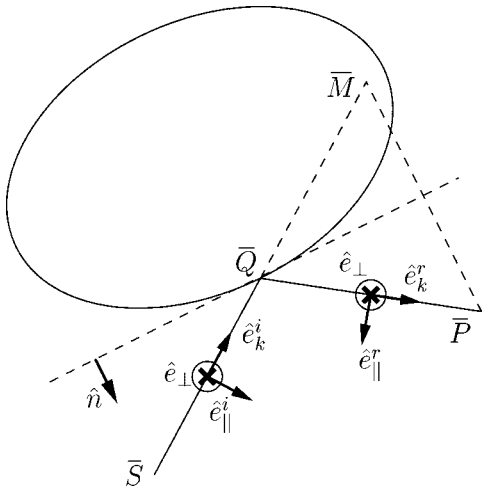

Fig. 1. Image point and vector definitions for reflection from a cylinder. The figure shows a cut in the plane of incidence.

We use a modification of this formulation. Consider the geometry shown in Fig. 1. The figure shows a cut in the plane of incidence, but the structure is, in general, three-dimensional. $\overline{S}$ is the source point and the point $\overline{M}$ is the mirror image of the field point $\overline{P}$ in the plane tangential to the cylinder surface at the specular point $\overline{Q}$

$$\overline{M} = \overline{P} - 2\hat{n}[\hat{n} \cdot (\overline{P} - \overline{Q})]$$

where $\hat{n}$ is the normal vector to the surface at $\overline{Q}$. In the absence of the scatterer the ray optical field at $\overline{M}$ may be found from a known field at $\overline{Q}$. Assuming spherical wave incidence, one finds

$$\overline{E}^i(\overline{M}) = \overline{E}^i(\overline{Q}) \frac{s^i}{s^i + s^r}\, e^{-jks^r} \quad (6)$$

which may be inverted to give the field at $\overline{Q}$ for a known field at $\overline{M}$. This may be substituted into (5) leading to

$$\begin{aligned} \overline{E}(\overline{P}) \approx{}& \overline{E}^i(\overline{P}) + \overline{E}^i(\overline{M}) \\ & \cdot \overline{\overline{\mathcal{R}}}\, \frac{s^i + s^r}{s^i} \sqrt{\frac{\rho_1^r \rho_2^r}{(\rho_1^r + s^r)(\rho_2^r + s^r)}} \end{aligned} \quad (7)$$

where the direct contribution $\overline{E}^i(\overline{P})$ is calculated at the original field point. In the case of reflection from a cylinder, $\rho_2^r = s^i$ and this equation simplifies to

$$\overline{E}(\overline{P}) \approx \overline{E}^i(\overline{P}) + \overline{E}^i(\overline{M}) \cdot \overline{\overline{\mathcal{R}}} \sqrt{\frac{\rho_1^r (s^i + s^r)}{s^i (\rho_1^r + s^r)}} \quad (8)$$

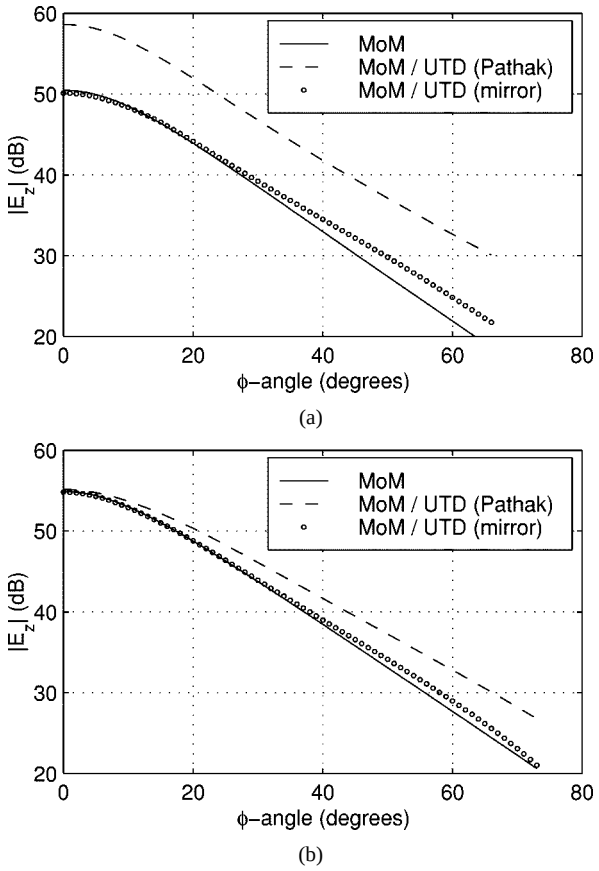

Fig. 2. The near field of a vertical Hertzian dipole in front of a cylinder with radius 1.5 λ. The field is calculated on a radius of 2.15 λ in the same plane as the source. The sources are (a) 0.1 λ and (b) 0.2 λ in front of the cylinder.

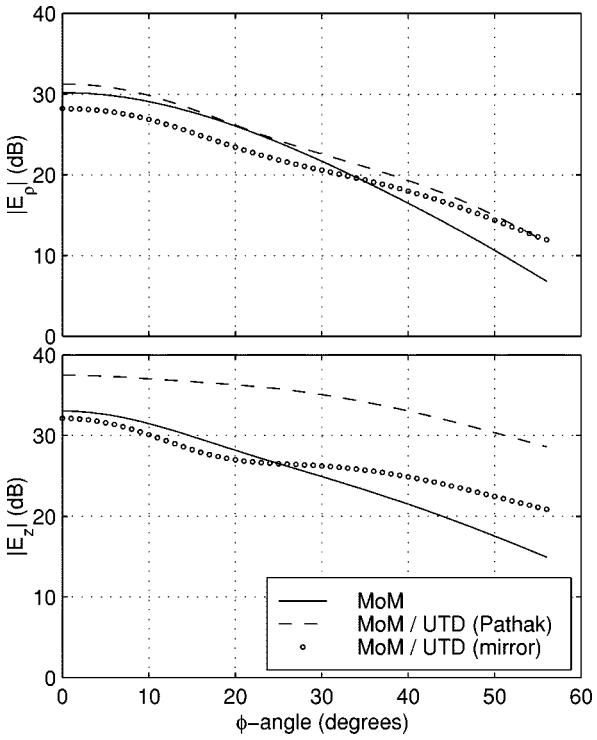

Fig. 3. The near field of a vertical Hertzian dipole 0.1 λ in front of a cylinder with radius 1.5 λ. The field is calculated on a radius of 1.85 λ in a plane 1 λ above the source.

which is valid in the entire lit region when the source and field points are such that the ray optical field approximation is valid.

Note that as $s^i \to 0$, $\rho_1^r \to s^i$ (provided that $\rho_1^r > 0$) and the term inside the square root tends toward unity. Near broadside the reflection coefficients $\mathcal{R}_{h,s} \to \pm 1$ and the tangential components at the field point $\overline{P}$ are the mirror image of those at the mirror point $\overline{M}$. (This is approximately what one would expect very close to a large cylinder.) In the other extreme, where the incident field is ray optical, our mirror formulation reduces to the original uniform GTD. Thus, we may argue that as (8) is physically consistent when the source and field points are in either the ray optical region or the very near region, we may use this equation throughout.

The reflection formulation is applied to the total field orthogonal to the direction of propagation (the components $\hat{e}_{\parallel}^{i,r}$ and $\hat{e}_{\perp}$). This field includes the near field terms ($1/r^2$ and $1/r^3$) in these directions *even though the reflection coefficients are derived for ray optical fields only*. This is a heuristic extension, but results presented in the next section show that it does indeed extend the "low-frequency" end of the GTD for specific problems of concern in a hybrid MoM/GTD code.

As ray optical fields do not have a component in the direction of propagation, the near-field component in this direction needs special treatment. We elect to treat this component as if mirrored in a infinite, perfectly conducting mirror. For near broadside reflections this will be similar to the GTD reflection coefficients which approach that of a flat plate. At the shadow boundary, the direction of propagation is tangential to the mirror plane. The direct and reflected contributions will thus cancel. This will be continuous with the creeping wave field diffracted into the shadow zone, as this formulation assumes a ray optical field that does not have a component in the direction of propagation.

The reflected field at $\overline{P}$ may thus be written as

$$\overline{E}^r(\overline{P}) \approx \overline{E}^i(\overline{M}) \cdot \overline{\overline{\mathcal{R}}}' \tag{9}$$

where

$$\overline{\overline{\mathcal{R}}}' = \sqrt{\frac{\rho_1^r(s^i + s^r)}{s^i(\rho_1^r + s^r)}} \left\{ \mathcal{R}_s \hat{e}_{\perp} \hat{e}_{\perp} + \mathcal{R}_h \hat{e}_{\parallel}^i \hat{e}_{\parallel}^r \right\} - \hat{e}_k^i \hat{e}_k^r \tag{10}$$

with $\hat{e}_k^i$ and $\hat{e}_k^r$ the unit vectors in the incident and reflected wave directions of propagation respectively as shown in Fig. 1. Note that the normal component of $\hat{e}_k^r$ (with respect to the tangential plane at $\overline{Q}$) is opposite to that of $\hat{e}_k^i$, while the tangential components are the same. Due to the negative sign of the second term in (10) the normal component is in the same direction as the field at $\overline{M}$, while the tangential component is opposite to it. For a magnetic boundary the sign of the second term becomes positive.

In the present implementation, the specular point and the ray directions are found for a spherical ray originating from the center of the source basis function in the MoM region with the field point at the center of the testing function.

IV. Numerical Examples

This section presents plots of the near field radiated by a Hertzian dipole very close to the cylinder as measure of the ac-

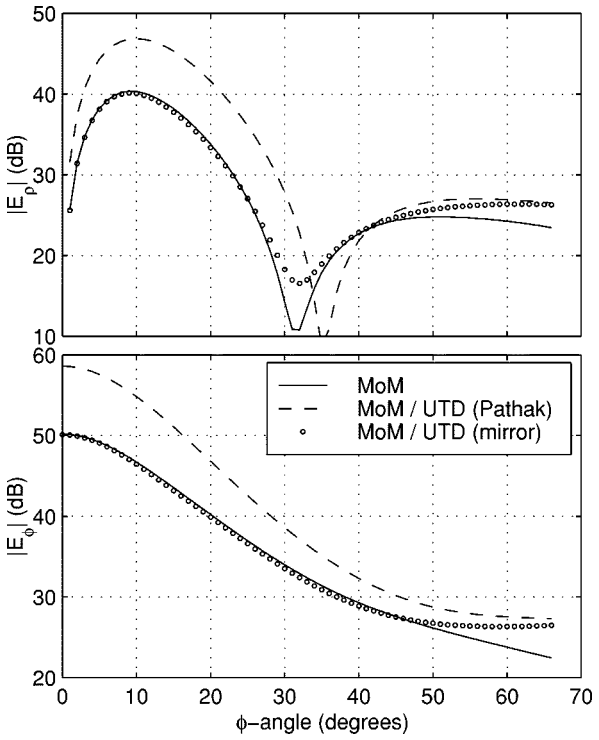

Fig. 4. The near field of a horizontal Hertzian dipole 0.1 λ in front of a cylinder with radius 1.5 λ. The field is calculated on a radius of 2.15 λ in the same plane as the source.

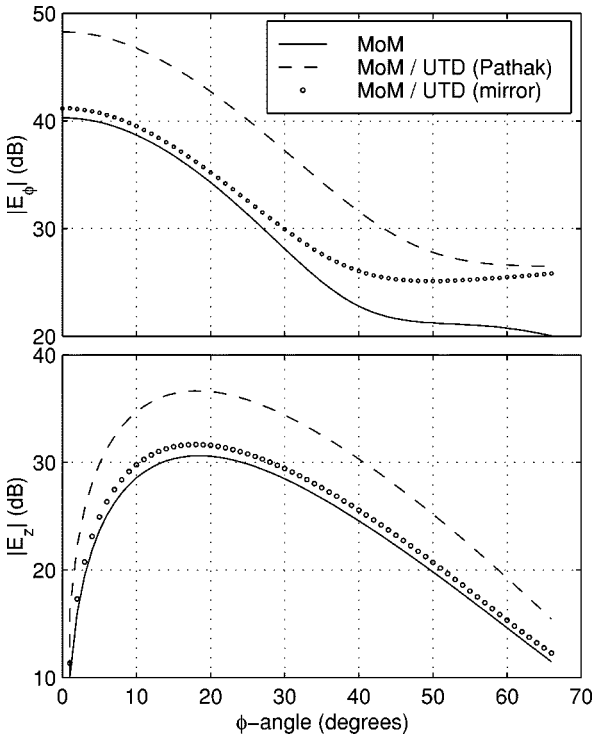

Fig. 5. The near field of a horizontal Hertzian dipole 0.1 λ in front of a cylinder with radius 1.5 λ. The field is calculated on a radius of 2.15 λ in a plane 1 λ above the source.

curacy and the region of validity of the mirror formulation. It also shows the input impedance of a half-wave dipole antenna as it is moved closer to a cylinder as an example of the application of the mirror formulation.

Figs. 2–5 show the near fields for a Hertzian dipole in front of a cylinder with radius 1.5 λ, sufficiently long that the end-cap effects may be ignored. The figures show the field strength in decibels with respect to 1 V/m when the Hertzian dipole amplitude $I\,dl$ is 1 Am. The MoM solution is given as a reference and is computed with a 16 λ long cylinder. We also show results which we have computed using the uniform GTD formulation due to Pathak *et al.* [3]. Note that this formulation is pushed beyond its intended limit in the examples shown here. This is done to indicate that the mirror formulation discussed above can improve the range of validity. The cylinder lies along the z-axis in cylindrical coordinates with the source at $\phi = 0^\circ$ and $z = 0$.

The two graphs in Fig. 2 show the near field pattern of a vertical (z-directed) dipole as a function of the cylindrical angle ϕ. In both cases the pattern is measured at a radius of 2.15 λ and $z = 0$ (in the same plane as the source). These curves, and all the other dipole patterns, are plotted up to the shadow boundary at about 70°, depending on the exact source and field radii. The graph in (a) shows the pattern for a source at a radius of 1.6 λ (only 0.1 λ in front of the cylinder) and shows clearly that the modified formulation yields much improved results. Note that the accuracy of the results decreases toward the shadow boundary. This may be expected from the fact that the component in the direction of propagation is ignored at this point. From the comparison in (b), it follows that a separation of 0.2 λ is almost large enough for the formulation [3] to be valid.

Fig. 3 shows the pattern on a radius of 1.85 λ, but in this case $z = \lambda$ such that the field also has ρ and ϕ components. We present only the two largest components. In this figure, it is clearly seen that the mirror formulation does not yield such a dramatic improvement. One reason is that the source and field points lie very close to the cylinder. With the much larger axial separation between them, the incident and reflected directions are very close to the cylinder axial direction. In this case, the angle of incidence approaches 90° while being far from the shadow boundary and the uniform GTD reflection coefficient does not remain valid. The case of horizontal (y-directed) dipoles is given in Figs. 4 and 5, both showing the fields on a radius of 2.15 λ, with the former on the same plane as the source and the second at $z = \lambda$. The same trend is evident. The horizontal polarization seems to be a little better behaved for small ϕ angles.

We have seen that the mirror formulation is most suspect when there is a large axial separation between the source and field points. Thus we have selected as a worst case application of this formulation a vertical (rather than horizontal) half-wave dipole (length 0.5 λ and wire radius 0.001 λ) in front of a cylinder of radius 1 λ. Fig. 6 shows the input impedance of the dipole as a function of the distance to the cylinder as an example of the application of this formulation. The plot compares the full MoM (which is used as a reference) to the hybrid formulation which uses MoM basis functions on the dipole segments and uniform GTD to incorporate the interaction with the cylinder. The figure shows that the uniform GTD theory due to Pathak *et al.* [3] starts diverging, as expected, for $d < 0.3\lambda$. The mirror formulation can be used much closer to the cylinder.

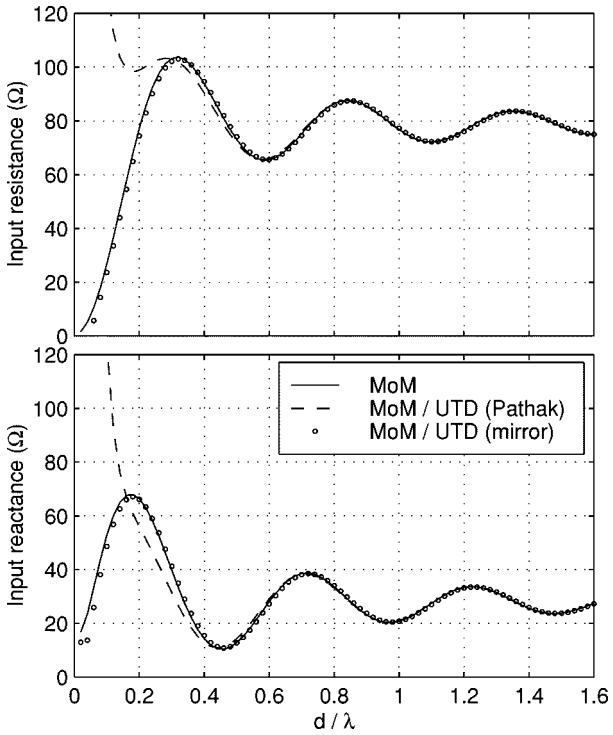

Fig. 6. Input impedance of a half-wave dipole (wire radius 0.001 λ) a distance d in front of a cylinder with radius λ. The dipole is parallel to the cylinder axis.

Very near to the cylinder this formulation also breaks down. This happens due to the breakdown of the uniform GTD on near axial directions, as well as the fact that one may no longer approximate the integral over the entire testing function in terms of the value at the center only. If plotted on the same scale, the input impedance of the horizontal half-wave dipole (not shown in this paper) only visibly diverts from the MoM solution at a spacing of 0.06 λ. This confirms the expectation that the result will be worse for a vertical dipole than for the horizontal one.

V. Conclusions

We have demonstrated an extension of the uniform GTD reflection formulation that considers the near field effects and can be easily implemented in a hybrid MoM/GTD code without having to model the basis functions in terms of Hertzian dipoles. It further enables the source to be very close to the cylinder provided that the source to reflection point to field point distance is not too short. We have seen that both the source and field point may be within 0.1 λ of the reflection surface, in this case provided that the axial separation is of the same order.

Acknowledgment

The authors would like to thank the staff of the Ohio State University ElectroScience Laboratory for some very useful discussions.

References

[1] G. A. Thiele and T. H. Newhouse, "A hybrid technique for combining moment methods with the geometrical theory of diffraction," *IEEE Trans. Antennas Propagat.*, vol. AP-23, pp. 62–69, Jan. 1975.

[2] U. Jakobus and F. M. Landstorfer, "A combination of current-and ray-based techniques for the efficient analysis of electrically large scattering problems," in *Proc. 13th Annu. Rev. Progress Appl. Computat. Electromagn.*, Monterey, CA, Mar. 1997, pp. 748–755.

[3] P. H. Pathak, W. D. Burnside, and R. J. Marhefka, "A uniform GTD analysis of the diffraction of electromagnetic waves by a smooth convex surface," *IEEE Trans. Antennas Propagat.*, vol. AP-28, pp. 631–642, Sept. 1980.

[4] P. H. Pathak, "High frequency techniques for antenna analysis," *Proc. IEEE*, vol. 80, pp. 44–65, Jan. 1992.

[5] H.-T. Chou, P. H. Pathak, and M. Hsu, "Extended uniform geometrical theory of diffraction solution for the radiation by antennas located close to an arbitrary, smooth, perfectly conducting, convex surface," *Radio Sci.*, vol. 32, pp. 1297–1317, July–Aug. 1997.

[6] R. F. Harrington, *Field Computation by Moment Methods*. New York: IEEE Press, 1993.

[7] M. Hsu, "Hybrid (MM-UTD) analysis of EM scattering by finned objects," Ph.D. dissertation, Dept. Elect. Eng., The Ohio State Univ., 1995.

[8] D. A. McNamara, C. W. I. Pistorius, and J. A. G. Malherbe, *Introduction To The Uniform Geometrical Theory Of Diffraction*. Norwood, MA: Artech House, 1990.

Isak P. Theron (S'88–M'95) was born in Upington, South Africa, in 1967. He received the B.Eng, M.Eng, and Ph.D. degrees from the University of Stellenbosch, South Africa, in 1989, 1991, and 1995, respectively.

After completing his doctorate on the electromagnetic characterization and numerical simulation of chiral materials, he spent a year (1996–1997) as a Visiting Scholar at the ElectroScience Laboratory, The Ohio State University, Columbus. Since returning to South Africa, he has been a Postdoctoral Associate at the University of Stellenbosch and is currently a Research Engineer at Electromagnetic Software and Systems (EMSS). He is currently working on the extending the high-frequency hybrid techniques within the FEKO CEM code.

Dr. Theron is a member of ACES.

David B. Davidson (M'86) was born in London, U.K., in 1961. He received the B.Eng, B.Eng (Hons), and M.Eng degrees from the University of Pretoria, South Africa, all *cum laude*, in 1982), 1983, and 1986, respectively, and the Ph.D. degree from the University of Stellenbosch, South Africa, in 1991.

Following national service (1984–1985) in the South African Defence Force (SADF), he worked at the Council for Scientific and Industrial Research (CSIR), Pretoria, before being appointed at the University of Stellenbosch in 1988. He is currently a Professor at that university. He has spent sabbaticals at the University of Arizona (1993), Tucson, and Cambridge University (1997), U.K., where he was a Visiting Fellow at Trinity College. He has published extensively on computational electromagnetics and recently served as Guest Editor for the *ACES Journal* special issue on high-performance computing and CEM. He is joint editor of the "EM Programmer's Notebook" column of the *IEEE Antennas and Propagation Magazine*.

Dr. Davidson received the (South African) FRD President's Award. He is a member of ACES and SAIEE and is past chairman of the IEEE AP/MTT Chapter of South Africa.

Ulrich Jakobus was born in Kirchheim/Teck, Germany, in 1967. He received the Dipl.Ing. and Dr.Ing. degrees in electrical engineering from the University of Stuttgart, Germany, in 1991 and 1994, respectively.

Since 1991, he has been with the Institut fur Hochfrequenztechnik, University of Stuttgart. In 1999 he completed his Habilitation and became Privatdozent at the University of Stuttgart. He has published extensively on computational electromagnetics and related topics. His main areas of research include numerical techniques in electromagnetics, antennas, electromagnetic compatibility, and bioelectromagnetics.

Dr. Jakobus is a member of URSI Commission B, several IEEE societies, the German VDE/ITG, and the Applied Computational Electromagnetics Society (ACES). He has received several awards for his research, including the ACES 1996 Outstanding Paper Award and the 1998 Heinz–Maier Leibnitz Prize by the Deutsche Forschungsgemeinschaft.